Solar-Driven Desalination System Using Two Types of Evacuated Tube Collectors

Zohreh Rahimi-Ahar[a*], Masoud Farghadani[b], Koroush Khosravi Darani[b], Mahdi Torabi[b]

[a] Department of Chemical Engineering, Engineering Faculty, Velayat University, Iranshahr, Iran.
Tel./fax: +98 5437211279

[b] Green Energies Technologists Company (Avisa), Isfahan, Iran.

Tel./fax: +98 3195026805

z.rahimi@velayat.ac.ir (Z. Rahimi-Ahar), S.forou@yahoo.com (M. Farghadani), Kkhdarani@gmail.com (K. Khosravi Darani), mahdii.torabii@gmail.com (M. Torabi)

Abstract

Desalination is an appropriate response to climate change, and increasing population, industrial activities, and drought. This study introduced a freshwater generation system using solar distillation via evacuated tube collectors (ETCs). Two geometries of evacuated tubes (Designs I and II) were used and the performance of the proposed system was evaluated regarding freshwater productivity, gained output ratio (GOR), and cost per liter (CPL). The difference between these tubes was the volume of the water circulating within them due to different internal geometries. The system benefitted from zero liquid discharge technology. Maximum freshwater productivity values of 1145 and 1325 $mL.h^{-1}.m^{-2}$ were obtained for Designs (I) and (II), respectively. It occurred in June 2023 under a maximum solar radiation intensity of 1010 $W.m^{-2}$. A maximum GOR of 0.71 and 0.82 was calculated at this peak solar radiation intensity for Designs (I) and (II), respectively. The quality of produced water met the standards of drinking water. The cost analysis led to the CPL of 0.0137 and 0.0132 US $ for Designs (I) and (II), respectively. The performance comparison of the proposed designs with other direct desalination units confirmed the superiority of these designs based on freshwater productivity, GOR, and CPL.

Keywords: Freshwater, Productivity, Evaporation, Gained Output Ratio, Cost

[*] Phone number: +989144261099

1. Introduction

The world population is growing at a quick rate, augmenting the drinkable water demand. Freshwater resources accessibility will be further stressed, with 2.3 billion more people than today experiencing severe water scarcity, especially in Africa, and Central and South Asia [1]. Desalination is the most proper process to decrease this stress by removing dissolved salts from water. Renewable energies (solar, geothermal, bioenergy, etc.,) are available in nature free of charge with no CO_2 footprint, which makes them the promising choices for desalination. Among them, the solar desalination process by a quick technological progression overcomes the rising freshwater demand at a reasonable cost, particularly on a small-scale desalination unit in remote areas [2].

Direct and indirect desalination processes are the classification of a solar desalination system. In the first system, desalination and energy collection are combined in one process, producing desalinated water by applying collected solar energy to saline water. The latter system comprises sub-systems of a solar collection unit (for collecting heat from the solar collectors and using it in a heat exchanger) and converting solar energy to power by the photovoltaic (PV) modules to run a desalination unit [3]. In some industries recovering the used water is critical. For example, city gate station gas heaters need continuous purified water. Small-scale humidification-dehumidification (HD) desalination units can recover freshwater from the waste heat of these gas heaters by thermosyphon heat pipe [4]. Another alternative is a pulsating heat pipe that recovers waste heat from a chimney to heat water [5]. Solar water heaters deliver hot water, while the produced hot water does not have the required quality for drinking. Hence, developing a household water desalter with high-quality water is worth developing water desalination technology [6]. Solar distillation using solar stills (basin type double slope, hemispherical, tubular, pyramid, triangular, and cascade) is categorized as active and passive distillation processes. In the first category, solar still (SS) absorbs direct sunlight as heat and water productivity is low. To increase water productivity, using phase change materials (PCMs), internal condenser, PV modules, proper insulation materials, noble and non-noble plasmonic nanoparticles, and integration with evacuated tube collectors (ETCs) and heat pipes [5,-7] have been proposed. Some desalination systems benefitting from ETCs are summarized as follows. A cogeneration system by productivities of freshwater via reverse osmosis (RO) and membrane distillation (MD) units, electricity using a turbine, and hot water via photovoltaic/thermal (PV/T) collectors as well as ETCs was analyzed using TRNSYS® [9]. The ETC surface, tilt angles of PV/T and ETC, the capacity of the water storage tank and batteries, and inlet water mass flow rates to the heater or/and the MD unit affected the system performance. The freshwater productivity of the MD unit was 15311 L/year. Coverage of solar water heater, overall freshwater productivity (including MD and RO), and power was 99.3%, 100%, and 70% which could be improved by system optimization. The 35% and 7% improvements in the generated electric energy and MD production were observed as compared to the base case. Wastewater was heated using a parabolic trough collector (PTC) and clean water was separated from pollutants in a modified SS [10]. A photodegradation process occurred when a galvanized ZnO plate was introduced into the still. This process enhanced the concentrate quality. A 93 % photodegradation of carmine dye was detected within 2 hours of the process. All these systems introduced coupling a solar water heater into a desalination unit to improve the desalinated water productivity.

Limited studies have been conducted on evaporation and heating processes in a stand-alone device. The performance of a solar-assisted hybrid hot water and desalinated water system (containing the heat storage device and superconducting gas double ETCs) was compared with a stand-alone desalination unit [11]. Operation at various heat storage temperatures of 50 °C to 70 °C and with no heat storage was examined. The increasing and decreasing trends were observed by raising the heat storage temperature. The hot and pure water productivities for 45 °C were higher than 386 $L.day^{-1}$ and 10138.7 $mL.day^{-1}$ on a sunny day. The estimated cost of pure and hot water was about 0.452 $¥.L^{-1}.m^{-2}$ and 0.013 $¥.L^{-1}.m^{-2}$, respectively. Shafii et al. [12] used two vacuum tubes for evaporation, hence, freshwater production. The highest desalination rate of 0.83 $L.m^{-2}.h^{-1}$ resulted from tubes installed at an inclination angle of 35° and an 80% filling of a tube with water. Filling the tubes with wool reached the production rate of 1.01 $L.m^{-2}.h^{-1}$. This study confirmed the importance of the water volume in the collectors. A PTC-type evaporator was used to improve the performance of a desalination system [13]. A maximum production rate and energy efficiency of 0.27 $L.m^{-2}.h^{-1}$ and 22% were obtained by replacing aluminum foils in the space between the heat pipe and the ETC to strengthen heat transfer from the collector to the heat pipe. Applying oil in this space reached the production rate and efficiency 0.933 $L.m^{-2}.h^{-1}$ and 65%, respectively. A point-focus PTC was designed for desalination of saline water [14]. The maximum productivity and energy efficiency of 1.5 $L.h^{-1}$ and 36.7% on a sunny day were measured under the highest solar radiation of 626.8 $W.m^{-2}$ and the absorber temperature of about 150.7 °C. Wind speed, air temperature, and feedwater salinity had no substantial effect on the production rate.

The concentrate of an RO unit with a total dissolved solids (TDS) of 15200 ppm was conducted to an ETC basin SS to show the feasibility of this integrated system for distilled water production. Some building mineral pumice was applied to prevent the large bubble formation at the bottom of the ETC. A cubic condenser was selected to enhance the freshwater volume due to doubling the contact area of the condenser and water vapor. This configuration decreased freshwater production (4.58±0.12 $L.m^{-2}$) by eight times compared to the configuration with one face contact area of the condenser and water vapor [15]. The response surface methodology (RSM) based on the Box-Behnken experiment design model was used for system optimization. The highest distilled water productivity (7.231 kg/m^2day) was obtained at a condenser wall thickness of 4 mm, a condenser volume of 2940 cm^3, and a condenser surface area of 0.336 m^2 [16]. An inclined weir-type SS was developed to improve the configuration of SS by increasing the aperture area. The best values of distance between weirs (3.5 cm), weir height (2 cm), and distance between the condenser cover and the absorber plate (15 cm) were obtained using the Box-Behnken experiment design model. The highest water production volume reached ~6.47 $kg.m^{-2}.day^{-1}$ [17]. The desalinated water productivity was directly influenced by the temperature difference between the solar desalination cover and the saline water [18]. Using black powder-coated crushed granite stone [19] and black iron oxide magnetic powder [20] as the absorbers of SS increased solar radiation absorption. These absorbers also showed a positive effect on energy storage, and energy and exergy efficiencies. The performance of an SS system could benefit from mirrors, waste material, and thermoelectric generators liberating heat from the absorber [21]. Integrating eccentric reflective solar collectors into single-effect absorption chillers and multi-objective optimization reduced the levelized cost of cooling. The cost-effectiveness enhanced by 29% compared to conventional solar-driven coolers [22].

The conventional SS was modified with five configurations of SS with no wick, blackened basin SS with a wick at 30°, and SS with a wick at 15°, 30°, and 45°. The performance of these configurations was compared at a constant water flow rate of 0.2 $g\ m^{-2}s^{-1}$ flowing through the basin and the wick. The blackened basin SS had the best performance by an embodied energy of 457.15 kWh, the highest freshwater productivity of 4.372 $kg.m^{-2}$, a minimum energy payback time of 1.11 years, and a distillate cost of ₹ 1.38 L^{-1} among its counterparts. The SS with 30°, 45°, and 15° wick obtained the next rankings regarding the freshwater productivity (4.25, 3.925, and 3.802 kg.m^{-2}) [23]. Integrating nano PCM using ZnO, CuO, Al_2O_3, Ag, graphene oxide, silica, carbon nanotube, graphite, carbon black, and graphene in the basin was recommended to increase the distillation yield [24]. Another strategy for improving the performance of solar-assisted desalination systems was the application of multi-criteria decision-making (MCDM) approaches namely measuring attractiveness by a categorical-based evaluation and weighted aggregated sum product assessment techniques [25]. ETCs were tested under different operating conditions. The volume fraction of water inside the tube significantly influenced the distiller output. The application of different tubes assisted in effective design benefitting from optimized water mass relative to the absorber tube area. Paraffin wax (a PCM) was used at two filling ratios of 100% and 50%, within the thermosyphon/pulsating heat pipe evacuated tube to show the effectiveness of this system considering the water production rate under low solar irradiation. The maximum freshwater production rate was 2248 mL/m^{-2} day^{-1}, showcasing a 40.7% rise in productivity compared to conventional SSs. SSs employing conventional and pulsating heat pipes exhibited an energy efficiency improvement of 19.4% and 20.3%, respectively [26].

This study introduced a freshwater generation unit using solar distillation via ETCs. Though solar water heaters have gained popularity for water heating in recent years, the study on desalination units using ETCs has rarely been experienced. Other studies have used one evacuated tube coupled to a condenser or several tubes integrated into an SS desalination system. The standard tubes (0.047 ID×1.765 m; Wall thickness: 1.7 mm) have been used for solar evaporation and solar water heating in vertically inclined mode. This study used the butterfly-shape arrangement of evacuated tubes. Moreover, two geometries of evacuated tubes (Designs I and II) were used. Design II benefitted from the newest geometry of tubes with lower water volume that have not been experienced for solar desalination. The performance of the system was evaluated regarding freshwater productivity, GOR, and CPL.

2. Process description

The experimental setup consisted of the main components of 40 ETCs (Evaporator), two heat exchangers (Preheater and Condenser), and saline and desalinated water tanks. Figs. 1 and 2 show the photograph and the 3D diagram of this setup. The saline water in the storage tank (1) flowed into a double-pipe heat exchanger (7). This heat exchanger preheated the feed saline water (2) while condensing the produced vapor (6). Preheating of feed water decreased the time required to close the circulating water temperature to the boiling point. Preheated water (3) flowed into the header (4) and distributed into the evacuated tubes (5). Water boiled and the produced vapor was directed from the header into the heat exchanger (7). The first stage of condensation occurred in this heat exchanger. Vapor was condensed using the feed saline water (2). For complete vapor condensation, the vapor was directed into the second heat exchanger (8) including six inclined pipes. Some part of these inclined pipes was integrated into fins to increase the heat transfer surface area. The inclined shape of the condenser allowed it to occupy less space while providing a high heat transfer area. The chimney-like shape also assisted in vapor suction into the condenser. The desalinated water (9) was collected in a storage tank (10). An appropriate inclination angle for these pipes was experimentally selected to maximize the condensation rate. Moreover, a slight inclination toward the header was made to create a slope for concentrated water leaving from each tube and preventing salt deposition inside each tube. Water filled the collectors and the water depth inside the ETCs was equal to the internal diameter of the tubes. Produced crystalline salt could be removed from the system after a while, considering the quality of feed saline water. This system benefitted from ZLD technology and no brine entered the environment. Two types of ETCs were used to evaluate an increase in the evaporation rate by reducing the volume of water flowing inside the evacuated glasses. Conventional ETCs were used in the first design while the second design benefitted from a new internal shape. The schematic of these tubes is presented in Fig. 3. The main differences between the proposed tubes were their inner length and internal geometry. These differences decreased the volume of water flowing into the collectors. Table 1 shows the list of the components and their characteristics. The collectors were installed at a yearly optimum tilt angle of 35° to achieve direct solar radiation. This value was selected considering the location of the experiments.

3. Material and methods

The brackish and saline water were synthesized by the addition of 10 and 35 g of sea salt into 1 kg of tap water, respectively.

The performance of the proposed system could be evaluated in terms of GOR. GOR shows the ratio of latent heat of produced distilled water to the energy input into the unit [27] and is defined as [28]:

$$\text{GOR} = \frac{\dot{m}_{pw}h_{fg}}{\dot{Q}_i} = \frac{\dot{m}_{pw}h_{fg}}{I.A} \quad (1)$$

Where, $\dot{m}_{pw}$, h_{fg}, $\dot{Q}, I$, and A are the freshwater production rate (kg.s^{-1}), specific enthalpy of evaporation (kJ.kg^{-1}), inlet heat (kW), solar radiation intensity (kW.m^{-2}), aperture area of the ETCs (m^2), respectively.

The produced water specification (conductivity, TDS, and pH), solar radiation intensity, and ambient temperature were recorded during the experimentation. The specifications of the measuring devices and their respective uncertainties in the experiments are shown in Table 2. The uncertainty values were of Type B and calculated by [29]:

$$u = \frac{a}{\sqrt{3}} \quad (2)$$

Where a and u are the accuracy and uncertainty, respectively.

The parameters and the ranges of the operating conditions are shown in Table 3. The system analysis was performed via one factor at a time approach using one quality- and three quantity-based parameters. Table 3 tabulates the solar radiation intensity, tilt angle of the ETCs, and water salinity varied within the ranges. Their effects on the desalination rate were investigated and the main parameters were determined. The saline water storage tank was equipped with a floater. Besides, the tank was installed on an equal level with the top row of the collectors. Applying a floater compensated for the water level reduction in the tubes due to the continuous water boiling and evaporation. Therefore, the inlet water mass flow rate was not an effective parameter. Boiling occurred in the collectors and the boiling point in the location of the experiment was 95 °C. On the other hand, the vacuum space between the inner and outer tubes prevented considerable heat loss. This caused no significant temperature difference between the inner glass and water.

4. Results and discussion

The tests were conducted under the climatological conditions of Isfahan, Iran (Longitude: 51.6680, Latitude: 32.6546) in June 2023. The average ambient temperatures and radiation intensities are presented in Fig. 4. The ambient temperature varied between 24 and 31 °C while the solar insolation ranged between 320-1010 W.m^{-2} during the days of experiments. The temperatures and radiation intensities increased until noon and then started to decrease. The tests were conducted on the 1st, 15th, and 29th of June and the average values of the desalination rate were registered.

4.1 Effect of the tube geometry on freshwater productivity and energy efficiency

The environmental conditions and solar intensity affect the process water temperature, hence, freshwater productivity. The evaporation rate strengthens and enhances the desalination rate by increasing the solar radiation intensity. The freshwater production rate per m^2 of solar collector aperture area ($mL.h^{-1}.m^{-2}$) is shown in Fig. 5. A longer time was required to boil the saltwater in the ETCs, vapor generation, and start the freshwater accumulation. So, zero productivity was observed before 11 and 11.30 a.m. for Designs (II) and (I). The experiments were conducted at a salinity of 3.5 wt.%.

As the water temperature in the absorber increased by an increase in the solar radiation intensity, the thermal capacity of the water decreased, causing an increase in the evaporation rate, therefore, reaching the maximum hourly production rate of about 1325 and 1145 $mL.h^{-1}.m^{-2}$ for Designs (II) and (I), respectively. These maximum values were obtained for Designs II and I at 1 and 1.30 p.m., respectively. Obtaining the maximum freshwater at different times was due to the difference in the water volume in the collectors. Decreasing the water volume (Design II) led to the improvement of freshwater productivity by 13.6%. The average accumulated water during the test days for Designs (II) and (I) were 21890 and 18895 $mL.day^{-1}$. This result confirmed the superior performance of Design (II) due to its lower circulated water volume. This means the radiated solar intensity is more effective against the volume of water provided by Design (II).

It was observed that the desalination rate increased by increasing the solar radiation intensity. It was at its highest value at noon, and thereafter, it lessened. This means the rate of freshwater production is in good agreement with the variation in the solar intensity during the test days.

A maximum desalination rate using Designs (I) and (II) is tabulated in Table 4. Maximum GOR was calculated at the maximum water production rate and solar radiation intensity. It ranged from 0.28 to 0.71 for design (I) and 0.33 to 0.82 for design (II). Furthermore, as the water volume in the glasses of Design (II) was lower than that in Design (I), its desalination rate was higher. About a 12.8% increase in the GOR was obtained via Design (II). This means lowering the volume of water flowing into the system enhances the performance of the system.

4.2 Effect of water salinity and tilt angle on freshwater productivity

The proposed systems were performed using brackish water and seawater with salinity values of 1% and 3.5%. Salinity lowers the saturation pressure of water and accordingly the saturation absolute humidity and saturation enthalpy of moist air. Salinity augments the specific heat at a constant pressure of the feed water. Hence, decreasing the freshwater productivity by increasing the salinity was expected.

The effect of salinity and inclination angle on freshwater productivity is presented in Fig. 6. It was concluded that the desalination rate decreased by about 4% as the salinity increased from 1% to 3.5%. However, this means the insignificance effect of salinity on the performance of this system. 5% salinity was also experienced to show the effectiveness of the proposed system in higher salinity water compared to the seawater. For a salinity of 5%, the freshwater productivity was about 2.8% lower than 3.5% salinity. Saline feed carries a risk of scaling that can greatly influence the operation in both designs after a while [30]. Periodic cleaning of the ETCs especially in design (II) due to its thick internal geometry should be considered.

The setup was tested at tilt angles of 25°, 35°, and 45° to confirm the effectiveness of solar radiation direction. The maximum productivity for Design (II) with the inclination angles of 25°, 35°, and 45° was about 958, 1325, and 1234 $kg.m^{-2}.h^{-1}$, respectively, showing the appropriateness of the inclination angle of 35°. By deviating the angle from 35° the normal radiation on the ETCs reduced, which lessened the freshwater productivity, accordingly.

4.3 Water quality analysis

The physicochemical properties of desalinated water are present in Table 5. The standard range is obtained from WHO guidelines for drinking water quality [31]. This analysis report confirms that the produced desalinated water in the proposed system has the characteristics of distilled water and can be drinkable by adding useful minerals. Notably, the lower concentration of Na^+, TDS, and EC values specify the presence of lower dissolved solids and henceforth, lower salinity for produced water due to desalination. Based on the WHO guidelines for the quality of drinking water [32], the TDS values of <600 $mg.L^{-1}$ are potable as they become non-potable at TDS levels of >1000 $mg.L^{-1}$.

4.4 Cost analysis

To assess the cost-effectiveness of a desalination unit and evaluate the unit cost of the produced water, a cost analysis was performed. The cost of water produced employing a desalination unit was determined using variable and fixed costs. No electrical devices were used in this system, hence, the cost related to electricity consumption was zero. The power consumption and energy costs in this system were zero. All prices were consistent with the Iranian market in 2023 in Rials that were changed to US$. The details of the CPL of the produced water and the investment cost in the proposed system are presented in Tables 6 and 7. The maintenance cost was considered 12% of the fixed capital cost per year [33] with a lifetime of 20 years [13].

The average daily desalination rates were about 18.9 and 21.8 $L.day^{-1}$ for Designs (I) and (II), respectively. Considering 300 sunny days of system run per year in Isfahan, the total desalinated water productivity during a year was 5691 and 6593 L for designs (I) and (II), respectively. According to these assumptions, the CPL was calculated.

The minimum CPL of 0.0137 and 0.0132 $\$.L^{-1}$ was attained considering the maximum freshwater production. The CPL would decrease to more reasonable values by coupling the proposed system with other desalination systems, enhancing the energy efficiency of the components, and scaling up the system. These values would increase and decrease on colder and warmer days during the year, respectively. Furthermore, the unit cost is decreased by applying more durable components. The CPL will be lower in areas with more solar radiation and longer sunny and clear days.

4.5 Performance comparison of different desalination systems

Freshwater productivity, GOR, and CPL were analyzed to compare the performance of the proposed system and other small-scale desalination systems containing ETC and PTC (Table 8). The heating and evaporation of saline water occurred in PTCs and ETCs. SSs were coupled to the solar collectors to increase the subjected radiated area. The comparison results can be summarized as follows:

- The proposed designs in this study benefitted from the most acceptable freshwater productivity, GOR, and CPL among its counterparts. Although, evaporation using ETC coupled with active SS had high freshwater productivity, energetic and cost analyses were not been reported to make a clear comparison. The proposed system, ETC coupled to active SS, ETC coupled with SS containing wick, ETC coupled to 5-effect SSs, vacuum evaporation using ETC, and PCM integrated SS systems placed in an appropriate position by >1000 $mL.h^{-1}.m^{-2}$ productivity. Integrating SS into the proposed system can be favorable. Most systems introduced in Table 8 benefitted from a cost range of 0.013-0.015 $\$.L^{-1}$. On the other hand, ETC coupled to SS and heat exchanger with a minimum cost of 0.0084 $\$.L^{-1}$ showed the positive effect of using an appropriate heat exchanger, hence, encouraging to development of an appropriate heat exchanger in our system.

- Using ETC with an appropriate water volume within the tubes improved the system's performance.

- Coupling multi-effect SS with the ETC-typed evaporator significantly increased the GOR of the system. Applying PCM in SS or appropriate wick to increase the energy storage capacity and heat transfer surface area was necessitated.

- Vacuum evaporation and increasing the number of PTCs and ETCs were recommended.

5. Challenges and recommendations for future research

The proposed system can be applied in arid areas facing drinkable water shortage, as produces sufficient freshwater for domestic uses. However, it suffers from energy storage and night-time operation. These problems can be overcome using PCMs. PCMs preserve solar energy during the night and improve the performance of desalination systems[45]. Heat pipe-type tubes containing high conductivity nanofluid can be another option [46]. Adding reflectors strengthens solar energy absorption and freshwater productivity [21]. The main source of error is freshwater production rate measurement. This causes wrongness in calculating freshwater productivity, GOR, and CPL. The best way to provide a reliable response is by using the design of the experiment (DOE) and the application of the RSM.

Coupling the proposed system with other desalination units (e.g., HD and multi-effect SS, etc.) and using their brine with a temperature of >40 °C shortens the initial time of freshwater production. This leads to starting the operation in the first of a day. Larger scale systems can be fabricated using PCMs and heat pipes in evacuated tubes. Integrating this unit with other desalination systems can provide drinkable water for semi-industrial applications. Furthermore, modification of the preheating section is recommended by adding a larger double-pipe heat exchanger or integrating SS to produce simultaneous hot and desalinated water.

6. Conclusion

This study introduced a desalination unit based on solar evaporation using ETCs. This technology could supply fresh water for people living in regions with saline and brackish water sources. Two geometries of evacuated tubes with different water volumes (Designs I and II) were tested under Isfahan weather conditions in June 2023. The effect of operational and environmental parameters on freshwater productivity was discussed. Water quality analysis showed the quality of produced water meets the standards of drinking water reported by the WHO. The proposed designs benefitted from ZLD technology. An economic analysis was conducted to assess the unit cost of the produced water. A summary of the obtained results is reported as follows:

- The most effective parameter on freshwater productivity was solar insolation.

- No significant effect of the salinity of the feeding water was observed.

- Designs (II) and (I) had a maximum desalination rate of 21890 and 18895 $mL.day^{-1}$, respectively.

- Maximum GOR of 0.82 and 0.71 was calculated at the peak solar radiation intensity for Designs (II) and (I), respectively.

- The cost analysis led to the CPL of 0.0132 and 0.0137 US $\$.L^{-1}$ for Designs (II) and (I), respectively. This unit possessed great economic value.

Conflict of interest

The authors declare that they have no conflict of interest.

Acknowledgment

This research did not receive any specific funding.

Data availability

Data will be made available on request.

References

[1] Pomázi, I. OECD Environmental Outlook to 2050. The Consequences of Inaction. Hungarian Geographical Bulletin, 61 (2012) 343-345.

[2] Ghaffour, N., Reddy, V.K., Abu-Arabi, M., Technology development and application of solar energy in desalination: MEDRC contribution, Renew. Sustain. Energy Rev. 15 (2011) 4410-4415. https://doi.org/10.1016/j.rser.2011.06.017.

[3] Wijewardane, S., Ghaffour, N. (2023). Inventions, innovations, and new technologies: Solar desalination, Sol. Compass. 5 (2023) 100037. https://doi.org/10.1016/j.solcom.2023.100037.

[4] Khalili, B., Kargarsharifabad H., Rahbar N., et al., Performance evaluation of a CGS gas heater-powered HDH desalination system using thermosyphon heat pipes: An experimental study with economic and environmental assessment, Int. Commun. Heat Mass Trans. 152 (2024) 107300. https://doi.org/10.1016/j.icheatmasstransfer.2024.107300.

[5] Shoeibi, S., Kargarsharifabad, H., Khiadani, M., et al., Techno-enviro-exergo-economic evaluation of hot water production by waste heat recovery using U-shaped pulsating heat pipe–an experimental study, Energy Sources, Part A: Recov. Utiliz. Environ. Effect. 46 (2024) 3292-3308. https://doi.org/10.1080/15567036.2024.2318005.

[6] Sasikumar, C., Manokar, A.M., Vimala, M., et al., Experimental studies on passive inclined solar panel absorber solar still, J. Therm. Anal. Calorimet. 139 (2020) 3649-3660. https://doi.org/10.1007/s10973-019-08770-z.

[7] Ahsan, A., Ahmad, N.S., Riahi, A., Uddin, M. A., Hridoy, D. N., Shafiquzzaman, M., Imteaz, M., Idrus, S., Al-Ansari, N., Atiq, M., Ng, A., Modeling of a new triangular shape solar distillation system integrated with solar PV panel and DC water heat heater. Case Stud. Therm. Eng. 44 (2023) 102843. https://doi.org/10.1016/j.csite.2023.102843.

[8] Gupta, A., Adithyan, T.R., Kalpathy, S.K., et al., Analysis of non-noble plasmonic enhanced solar distillation using computed optical activities, Desalination 541 (2022) 115999. https://doi.org/10.1016/j.desal.2022.115999.

[9] Acevedo, L., Uche, J., Del Almo, A., et al., Dynamic simulation of a trigeneration scheme for domestic purposes based on hybrid techniques, Energies 9 (2016) 1013. https://doi.org/10.3390/en9121013.

[10] Brito, E.T., Díaz, C.B., Córdoba, L.Á., et al., Evaluation of the efficiency of water treatment by a solar heating and distillation system, Environ. Challeng. 11 (2023) 100691.

https://doi.org/10.1016/j.envc.2023.100691.

[11] Zhou, X., Wu, L., Xiao, G., et al., Experimental investigation and economic analysis on a solar pure water and hot water hybrid system. Appl. Therm. Eng. 195 (2021) 117182. https://doi.org/10.1016/j.applthermaleng.2021.117182.

[12] Shafii, M.B., Mamouri, S.J., Lotfi, M.M., et al., A modified solar desalination system using evacuated tube collector, Desalination 396 (2016) 30-38. https://doi.org/10.1016/j.desal.2016.05.030.

[13] Mosleh, H.J., Mamouri, S.J., Shafii, M.B., et al., A new desalination system using a combination of heat pipe, evacuated tube and parabolic trough collector, Energy Convers. Manag. 99 (2015) 141-50. https://doi.org/10.1016/j.enconman.2015.04.028.

[14] Gorjian, S., Ghobadian, B., Hashjin, T.T., et al., Experimental performance evaluation of a stand-alone point-focus parabolic solar still, Desalination 352 (2014) 1-17. https://doi.org/10.1016/j.desal.2014.08.005.

[15] Samimi, M., Moghadam, H., Modified evacuated tube collector basin solar still for optimal desalination of reverse osmosis concentrate. Energy 289 (2024) 129983. https://doi.org/10.1016/j.energy.2023.129983.

[16] Moghadam, H., Samimi, M., Effect of condenser geometrical feature on evacuated tube collector basin solar still performance: Productivity optimization using a Box-Behnken design model. Desalination 542 (2022) 116092. https://doi.org/10.1016/j.desal.2022.116092.

[17] Samimi, M., Moghadam, H., Investigation of structural parameters for inclined weir-type solar stills. Renew. Sustain. Energy Rev. 190 (2024) 113969. https://doi.org/10.1016/j.rser.2023.113969.

[18] Shoeibi, S., Kargarsharifabad,H., Khiadani, M., et al., Techniques used to enhance condensation rate of solar desalination systems: State-of-the-art review, Int. Commun. Heat Mass Trans. 159 (2024) 108164. https://doi.org/10.1016/j.icheatmasstransfer.2024.108164.

[19] Dhivagar, R., Shoeibi, S., Kargarsharifabad, H., et al., Performance analysis of solar desalination using crushed granite stone as an energy storage material and the integration of solar district heating, Energy Sources Part A: Recov. Utiliz. Environ. Effect. 46 (2024)

1370-1388. https://doi.org/10.1080/15567036.2023.2299693.

[20] Dhivagar, R., Shoeibi, S., Kargarsharifabad, H., et al., Performance enhancement of a solar still using magnetic powder as an energy storage medium-exergy and environmental analysis, Energy Sci. Eng. 10 (2022) 3154-3166. https://doi.org/10.1002/ese3.1210.

[21] Shoeibi, S., Saemian, M., Parsa, S.M., et al., A novel solar desalination system equipped with thermoelectric generator, reflectors and low-cost sensible energy-storage for co-production of power and drinking water, Desalination 567 (2023) 116955. https://doi.org/10.1016/j.desal.2023.116955.

[22] Teles, M.P.R., Sadi, M., Ismail, K.A., et al., Cooling supply with a new type of evacuated solar collectors: a techno-economic optimization and analysis, Environ. Sci. Pollut. Res. 31 (2024) 18171-18187. https://doi.org/10.1007/s11356-023-25715-0.

[23] Negi, A., Verma, R.P., Saxena, A., et al., Design and performance of black painted Khes wick modified solar still: An experimental and 5E analysis, Int. J. Thermofluid. 20 (2023) 100491. https://doi.org/10.1016/j.ijft.2023.100491.

[24] Negi, A., Ranakoti, L., Bhandari, P., et al., Thermo-physical characteristics and storage material compatibility in nano-enhanced phase change materials for solar distillation applications: A critical assessment, Sol. Energy Mater. Sol. Cells 271 (2024) 112870. https://doi.org/10.1016/j.solmat.2024.112870.

[25] Singh, T., Entropy weighted WASPAS and MACBETH approaches for optimizing the performance of solar water heating system, Case Stud. Therm. Eng. 53 (2024) 103922. https://doi.org/10.1016/j.csite.2023.103922.

[26] Hemmatian, A., Kargarsharifabad, H., Esfahlani, A.A., et al., Improving solar still performance with heat pipe/pulsating heat pipe evacuated tube solar collectors and PCM: An experimental and environmental analysis, Sol. Energy 269 (2024) 112371. https://doi.org/10.1016/j.solener.2024.112371.

[27] Harby, K., Alsaman, A.S., Ali., E.S., Innovative and efficient integrations of desalination plants coupled absorption, adsorption, and humidification-dehumidification desalination units employing external heat recovery techniques, Energy Convers. Manag. 314 (2024) 118667. https://doi.org/10.1016/j.enconman.2024.118667.

[28] Pourghorban, F., Rahimi-Ahar, Z., Hatamipour, M.S., Performance evaluation of bubble column humidifier using various air distributors in a humidification-dehumidification desalination plant, Appl. Therm. Eng. 227 (2023) 120392. https://doi.org/10.1016/j.applthermaleng.2023.120392.

[29] Ayati, E., Rahimi-Ahar, Z., Hatamipour, et al., Water productivity enhancement in variable pressure humidification dehumidification (HDH) desalination systems using heat pump, Appl. Therm. Eng. 160 (2019) 114114. https://doi.org/10.1016/j.applthermaleng.2019.114114.

[30] McGovern, R.K., Thiel, G.P., Prakash Narayan, G., et al., Performance limits of zero and single extraction humidification-dehumidification desalination systems, Appl. Energy 102 (2013) 1081–1090. https://doi.org/10.1016/j.apenergy.2012.06.025.

[31] World Health Organization. Guidelines for drinking-water quality (Vol. 1). World Health Organization. ISBN 978 92 4 154760 4., 2004.

[32] Hanson, A., Zachritz, W., Stevens, K., et al., Distillate water quality of a single-basin solar still: laboratory and field studies, Sol. Energy 76 (2004) 635-645. https://doi.org/10.1016/j.solener.2003.11.010.

[33] Shafii, M.B., Jafargholi, H., Faegh, M., Experimental investigation of heat recovery in a humidification-dehumidification desalination system via a heat pump, Desalination 437 (2018) 81-88. https://doi.org/10.1016/j.desal.2018.03.004.

[34] Omidi, B., Rahbar, N., Kargarsharifabad, H., et al., Performance evaluation of a solar desalination-hot water system using heat pipe vacuum tube parabolic trough solar collector–An experimental study with Taguchi analysis, Energy Convers. Manag. 292 (2023) 117347. https://doi.org/10.1016/j.enconman.2023.117347.

[35] Dawood, M.M.K., Nabil, T., Kabeel, A.E., et al., Experimental study of productivity progress for a solar still integrated with parabolic trough collectors with a phase change material in the receiver evacuated tubes and in the still, J. Energy Storag. 32 (2020) 102007. https://doi.org/10.1016/j.est.2020.102007.

[36] Farghaly, M.B., Alahmadi, R.N., Sarhan, H.H., et al., Experimental study of simultaneous effect of evacuated tube collectors coupled with parabolic reflectors on traditional single

slope solar still efficiency, Case Stud. Therm. Eng. 49 (2023) 103304. https://doi.org/10.1016/j.csite.2023.103304.

[37] Singh, R.V., Kumar, S., Hasan, M.M., et al., Performance of a solar still integrated with evacuated tube collector in natural mode, Desalination 318 (2013) 25-33. https://doi.org/10.1016/j.desal.2013.03.012.

[38] Sampathkumar, K., Senthilkumar, P., Utilization of solar water heater in a single basin solar still-An experimental study, Desalination 297 (2012) 8-19, https:// doi.org/10.1016/j.desal.2012.04.012.

[39] Omara, Z.M., Eltawil, M.A., Elnashar, E.A., A new hybrid desalination system using wicks/solar still and evacuated solar water heater, Desalination 325 (2013) 56-64, https://doi.org/10.1016/j.desal.2013.06.024.

[40] Bhargva, M., Yadav, A., Experimental comparative study on a solar still combined with evacuated tubes and a heat exchanger at different water depths, Int. J. Sustain. Eng. 13 (2020) 218-229. https://doi.org/10.1080/ 19397038.2019.1653396.

[41] Gopi, G., Premalatha, M., Arthanareeswaran, G., Transient mathematical modelling and investigation of radiation and design parameters on the performance of multi-effect solar still integrated with evacuated tube collector, Energy Conversion and Mang.: X. 14 (2022) 100210. https://doi.org/10.1016/j.ecmx.2022.100210.

[42] Panchal, H.N., Enhancement of distillate output of double basin solar still with vacuum tubes, J. King Saud Univ. Eng. Sci. 27 (2015) 170-175. https://doi.org/10.1016/j.jksues.2013.06.007.

[43] Abbaspour, M.J., Faegh, M., Shafii, M.B., Experimental examination of a natural vacuum desalination system integrated with evacuated tube collectors, Desalination 467 (2019) 79-85. https://doi.org/10.1016/j.desal.2019.06.004.

[44] Faegh, M., Shafii, M.B., Experimental investigation of a solar still equipped with an external heat storage system using phase change materials and heat pipes, Desalination 409 (2017) 128-135. https://doi.org/10.1016/j.desal.2017.01.023.

[45] Rahimi-Ahar, Z., Khiadani, M., Rahimi Ahar, L., et al., Performance evaluation of single stand and hybrid solar water heaters: a comprehensive review, Clean Technol. Environm.

Policy. 25 (2023) 2157-2184. https://doi.org/10.1007/s10098-023-02556-6.

[46] Eidan, A.A., Alsahlani, A., Alshukri, M.J., et al., Experimental investigation of a solar evacuated tube collector embedded with a heat pipe using different nanofluids and controlled mechanical exciting pulsations, Int. J. Thermofluids. 20 (2023) 100415, https://doi.org/10.1016/j.ijft.2023.100415.

Caption of figures

Fig. 1. Photo of the proposed desalination unit

Fig. 2. 3D diagram of the proposed desalination system (1. Saline water storage tank, 2. Feed water pipe before preheating, 3. Preheated water pipe, 4. Header, 5. Evacuated tube collectors, 6. Vapor line, 7. Double-pipe heat exchanger, 8. Fin-equipped condenser, 9. Desalinated water line, 10. Desalinated water tank)

Fig. 3. Two geometries of the evacuated tubes in studied desalination system

Fig. 4. The variation of the ambient temperature and solar radiation intensity during test days (June 2023)

Fig. 5. The freshwater productivity (a) Design (I) and (b) Design (II) (3.5% salinity, 35° tilt angle)

Fig. 6. The effects of inclination angle and feed water salinity on freshwater productivity

Caption of tables

Table. 1. The components of water heating and desalination system and their characteristics

Table. 2. Specification of instrumentations used in the water heating and desalination system

Table. 3. Parameters and ranges of the operating conditions in the proposed co-production system

Table. 4. Performance evaluation of the proposed system based on the desalination rate and GOR using two designs of the tubes (3.5% salinity, 35° tilt angle)

Table. 5. Physicochemical properties of desalinated water

Table. 6. Investment cost of the proposed desalination system

Table. 7. Cost analysis proposed co-production system (at maximum solar radiation)

Table. 8. Performance comparison of the various small-scale desalination systems

Fig. 1. Photo of the proposed desalination unit

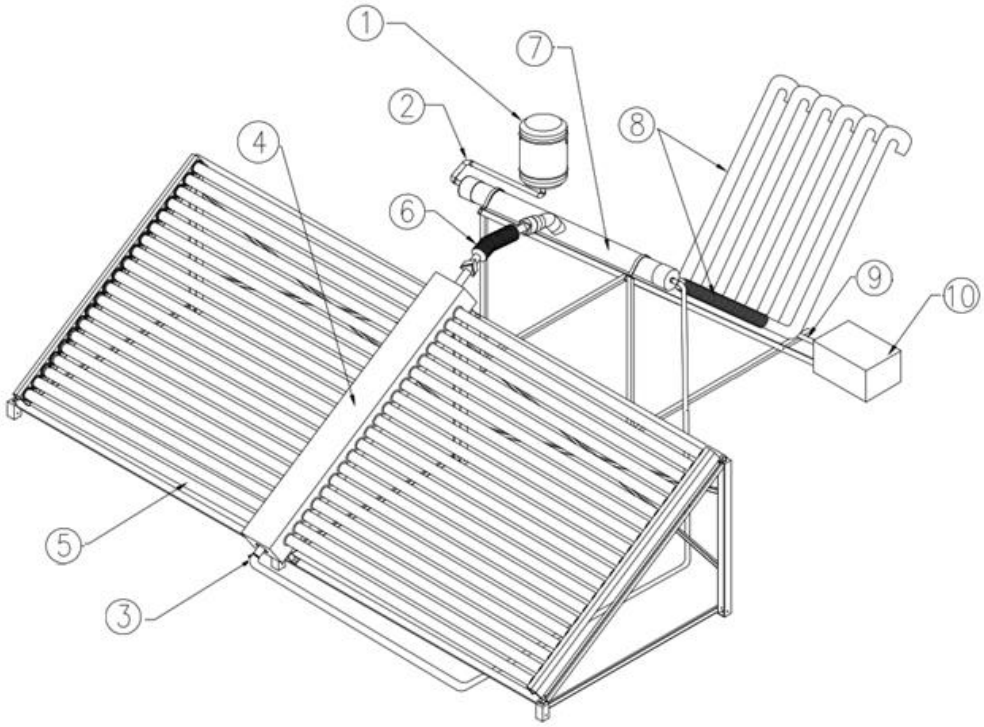

Fig. 2. 3D diagram of the proposed desalination system (1. Saline water storage tank, 2. Feed water pipe before preheating, 3. Preheated water pipe, 4. Header, 5. Evacuated tube collectors, 6. Vapor line, 7. Double-pipe heat exchanger, 8. Fin-equipped condenser, 9. Desalinated water line, 10. Desalinated water tank)

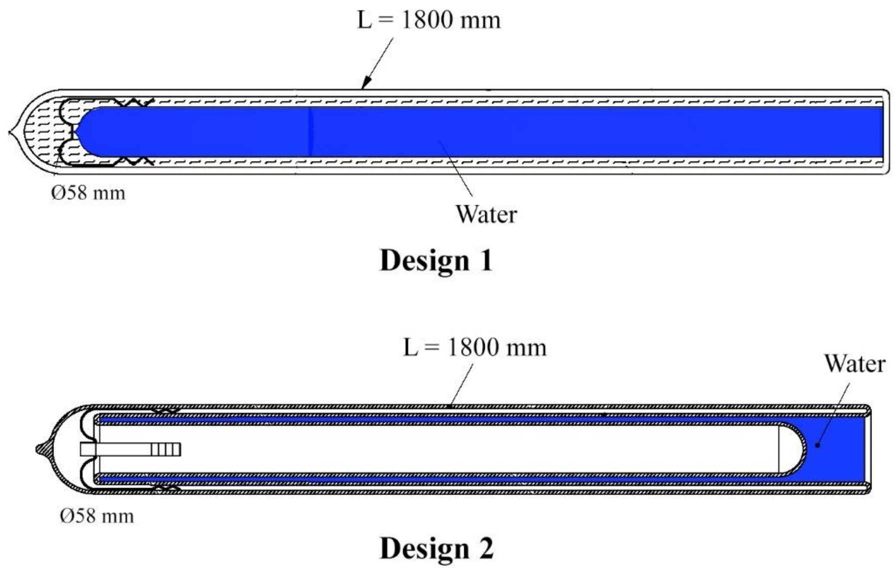

Fig. 3. Two geometries of the evacuated tubes in studied desalination system

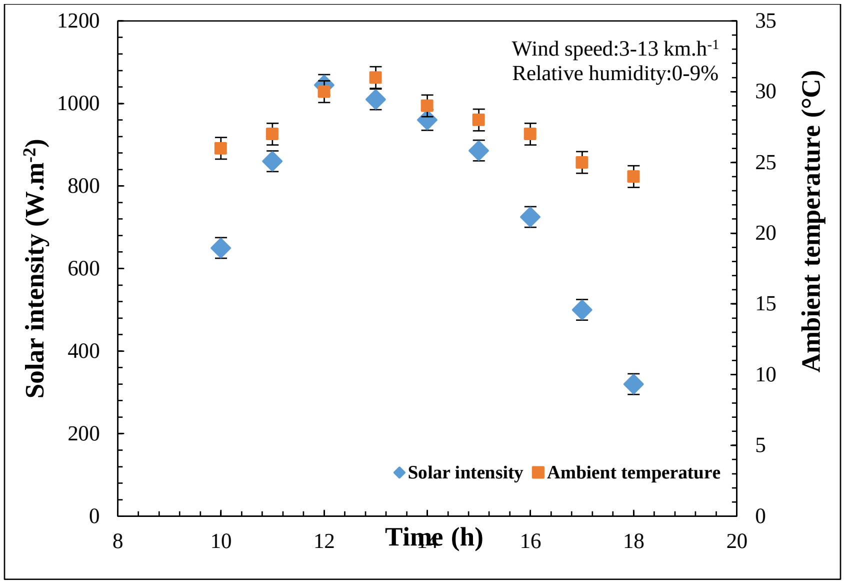

Fig. 4. The variation of the ambient temperature and solar radiation intensity during test days (June 2023)

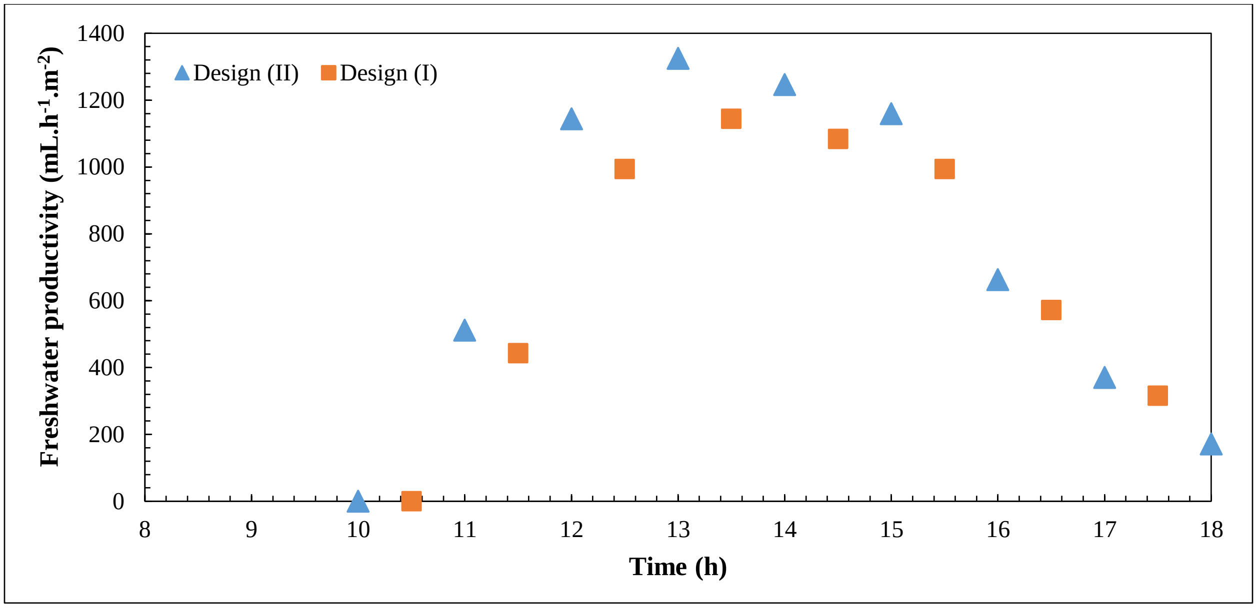

Fig. 5. The freshwater productivity (a) Design (I) and (b) Design (II) (3.5% salinity, 35° tilt angle)

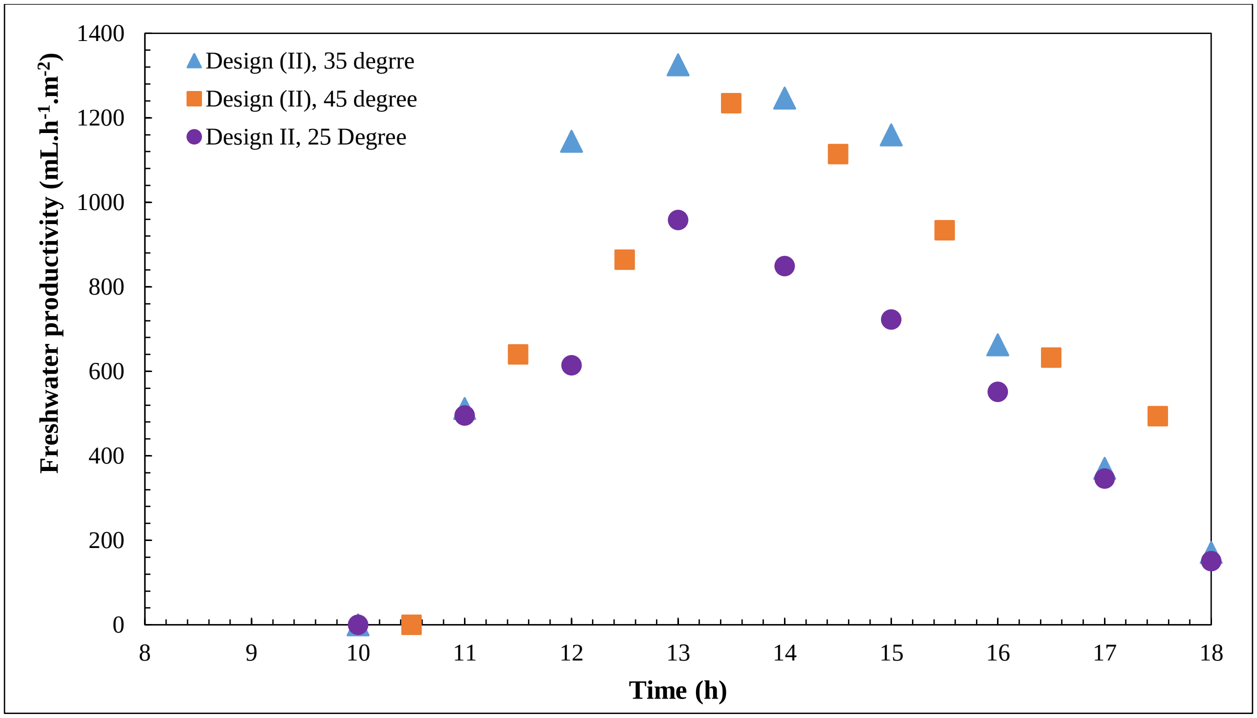

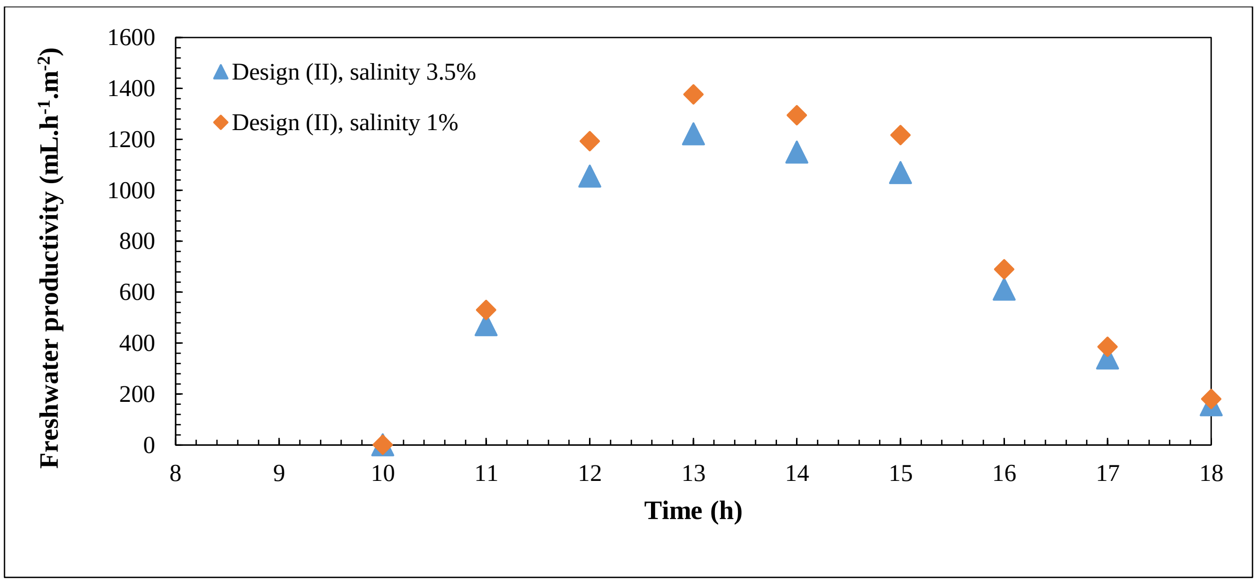

Fig. 6. The effects of inclination angle and feed water salinity on freshwater productivity

Table. 1. The components of water heating and desalination system and their characteristics

Component	**Description**	
Tank for desalinated water storage	Capacity: 50 L	
Tank for saline water storage	Capacity: 100 L	
Fin-equipped air condenser	6 inclined pipes: 0.051 OD×1.8 m	
Solar collector	40 glasses Header (0.19 ID×1.8 m); Water capacity: 47 L Aperture area: 3.32 m^2	
	Design (I)	**Design (II)**
	Cover Tube: 0.058 OD×1.8 m; Wall thickness: 1.8 mm **Inner Tube:** 0.047 ID×1.765 m (3 L); Wall thickness: 1.6 mm Total water storage capacity of glass tubes: 3×40=120 L	**Cover Tube:** 0.058 OD×1.8 m; Wall thickness: 1.8 mm **Inner Tube:** 0.047 ID×1.765 m; Wall thickness: 1.7 mm **Lining Tube:** 0.037 ID×1.465 m (1.57 L); Wall thickness: 1.5 mm Water storage capacity of glass tubes: 1.42×40=56.8 L

Table. 2. Specification of instrumentations used in the water heating and desalination system

Instrument	Range (unit)	Accuracy	Uncertainty (unit)
Solar meter (TES 132, Taiwan)	0 to 2000 ($W.m^{-2}$)	±1.0	0.6 ($W.m^{-2}$)
Conductivity meter (HM Digital Company, Korea)	0–9990 ($\mu S.cm^{-1}$)	±2.0 %	1.18 ($\mu S.cm^{-1}$)
pH meter (MW150 MAX, MILWAUKEE Company, USA)	0–14.0	±0.1	0.06
Water flowmeter (LUNA, Turkey)	0 to 1000 ($mL.min^{-1}$)	±20.0	11.8 ($mL.min^{-1}$)

Table. 3. Parameters and ranges of the operating conditions in the proposed co-production system

Parameters	**Range**
Solar radiation intensity	320-1010 W.m^{-2}
Water salinity (S_s)	1-3.5 %
Tilt angle	25-45°
Evacuated tube type	Designs (I) and (II)

Table. 4. Performance evaluation of the proposed system based on the desalination rate and GOR using two designs of the tubes (3.5% salinity, 35° tilt angle)

		Month
		June
Design (I)	Maximum desalination rate ($L.h^{-1}$)	3.8
	GOR	0.71
Design (II)	Maximum desalination rate ($L.h^{-1}$)	4.4
	GOR	0.82

Table. 5. Physicochemical properties of desalinated water

Parameter	**Unit**	**Value**	**Standard values for drinking water Ref.** [31]
pH	-	7.6	6.5-9
Total dissolved solids (TDS)	$mg.L^{-1}$	33	<1000
Cl^-	ppm	10.6380	<250
Ca^{+2}	ppm	2.0040	<300
Mg^{+2}	ppm	0.0000	<30
Na^+	ppm	2.3000	<200
Hardness	$mg.L^{-1}$	120	<300
Electric Conductivity (EC) at 25 °C	$\mu S.cm^{-1}$	51	N.A

Table. 6. Investment cost of the proposed desalination system

Description		**Cost (US $)**
Storage tank for desalinated water		10
Storage tank for saline water		20
Solar collector	Design (I)	80
	Design (II)	180
Header		100
Condenser		110
Pipes, fittings, and valves		60
Structural support		110
Total	Design (I)	490
	Design (II)	570

Table. 7. Cost analysis proposed co-production system (at maximum solar radiation)

Parameter (unit)	**Ref.**	**Description**	**Design I**	**Design II**
m (year)	[13]	Lifetime	20	20
i (%)	[33]	Interest rate	12	12
IC ($)	-	Initial cost	490	570
S = 0.2 × IC ($)	[33]	Salvage value	98	114
$AF = i (1+i)^m / [(i+1)^m - 1]$		Amortization factor	0.133	0.133
$SFF = i / [(i+1)^m - 1]$		Sinking fund factor	0.056	0.056
FYC = IC × AF ($)		First yearly cost	68.28	76.31
YS = SFF × S ($)		Yearly salvage	0.55	0.64
YMC ($) = 0.15 FYC		Yearly maintenance cost	10.24	11.45
YC = FYC + YMC − YS ($)		Yearly production cost	77.97	87.12
YY (L)	-	Yearly yield	5691	6593
CPL=YC/YY ($\$.L^{-1}$)	[33]	Yearly (cost/ yield)	0.0137	0.0132

Table. 8. Performance comparison of the various small-scale desalination systems

Description of system	**Max. freshwater productivity $mL.h^{-1}.m^{-2}$**	**Max. GOR**	**Min. Cost**	**Ref.**
Evaporation using PTC	750	0.751	0.0380 $\$.L^{-1}$	[34]
Evaporation using two PTCs coupled to a SS	815	0.34	0.0154 $\$.L^{-1}$	[35]
Evaporation using PTC coupled with SS	200	0.21	0.0235 $\$.L^{-1}$	[36]
Evaporation using ETC coupled with SS	168	0.544	-	[37]
Evaporation using ETC coupled with active SS	1460	-	-	[38]
Evaporation using ETC coupled with passive SS	720	-	-	
Evaporation using ETC coupled with SS containing double layers square wick	~1000	-	0.027 $\$.L^{-1}$	[39]
Evaporation using ETC coupled with SS	~230 $mL.h^{-1}$	-	0.0136 $\$.L^{-1}$	[40]

Evaporation using ETC coupled with SS and heat exchanger		$487\ mL.h^{-1}$		0.0084 $\$.L^{-1}$	
Evaporation using ETC coupled with 5-effect SSs		1192	3.19	-	[41]
Evaporation using ETC coupled with 2-effect SSs		850	-	0.26 $\$.L^{-1}$	[42]
Vacuum evaporation using ETC		1134	~ 0.65	0.0940 $\$.L^{-1}$	[43]
Evaporation using ETC coupled with SS		680	-	0.021245 $\$.L^{-1}.m^{-2}$	[44]
Evaporation using ETC coupled with SS added to a heat storage system		~650		0.026645 $\$.L^{-1}.m^{-2}$	
Evaporation using ETC coupled with Paraffin wax integrated into insulated SS		1025		0.013777 $\$.L^{-1}.m^{-2}$	
Evaporation using ETC coupled with Paraffin wax integrated SS		~1050		0.01527 $\$.L^{-1}.m^{-2}$	
Evaporation using ETC	Tubes with decreased water volume	1010	0.656	0.0142 $\$.L^{-1}.m^{-2}$	[11]
	Conventional tubes	830	0.526	0.0147 $\$.L^{-1}.m^{-2}$	

Evaporation using ETC	Design (I)	1145	0.71	0.0137 $\$.L^{-1}$	Present study
	Design (II)	1325	0.82	0.0132 $\$.L^{-1}$	

Biography

Zohreh Rahimi-Ahar, PhD, is a full-time Assistant Professor in the chemical engineering department of Velayat University, Iranshahr, Iran. She obtained her PhD degree in chemical engineering from the University of Isfahan in October 2018. Her activities focused on experimental studies of desalination systems and the development of process simulation and modeling. She has more than 15 papers on desalination systems in high-ranking journals. By combining these investigations, she aims to gain a comprehensive understanding of the chances of water desalination systems' development and environmental protection.

Masoud Farghadani is the CEO of Green Energies Technologists Company. He obtained his MS degree in Mechanical Engineering from the Isfahan University of Technology in Feb. 1992. His activities are focused on developing solar-assisted heating and desalination systems. He patented two solar-assisted heating and desalination units in 2016 and 2024. His current research deals with simultaneous desalination and hot water production based on solar energy.

Koroush Khosravi Darani, PhD, is the manager of Green Energy Technologists Company's solar desalination water production unit. He obtained his PhD degree in chemistry from the University of Isfahan in 2004. His activities focused on experimental studies of solar desalination systems.

Mahdi Torabi, a Mechanical engineer, is the research and development manager at Green Energies Technologists Company. He started his research on solar heating systems in 2013. In 2024, he patented a solar-assisted desalination and hot water production system. He continues his research on modifying the current desalination system.